J Mater Sci: Mater Electron (2017) 28:2069–2074
DOI 10.1007/s10854-016-5768-7

Structure and magnetic properties of CuO-substituted Co_2Y hexaferrites for high frequency applications

Xinyi Li[1] · Yu Wang[1] · Qian Liu[1] · Chongsheng Wu[1] · Qianqian Zeng[1] · Jie Li[1] · Yingli Liu[1]

Received: 28 July 2016 / Accepted: 1 October 2016 / Published online: 14 October 2016

Abstract In this paper, Cu-substituted Y-type hexaferrite $Ba_2Co_{2-x}Cu_xFe_{12}O_{22}$ (x = 0.0, 0.2, 0.4, 0.6, 0.8) materials were prepared by solid state reaction method. The structure and magnetic properties of ferrite have been investigated. CuO substitution not only adjusted structure and magnetic properties of sample, but also lowered sintering temperature. CuO modification endowed Co_2Y hexaferrites with better magnetic properties: dense microstructure, appropriate saturation magnetization, low coercivity and high permeability in high frequency. Light CuO improved grain morphology, when CuO was added from 0.0 to 0.8, saturation magnetization increased from 31.7 emu/g (x = 0.0) to 32.3 emu/g (x = 0.2), and then decreased to 27.74 emu/g (x = 0.8). Meanwhile, coercivity decreased from 172 Oe to 136 Oe with x from 0.0 to 0.8. The real part of magnetic permeability increased from 1.88 to 2.85 with Cu substitution. The imaginary part increased kept less than 0.25 and magnetic loss kept low value of 0.08 at 0.1–1 GHz frequencies. DC resistivity of the ferrites first increased from 3.65×10^5 Ω cm (x = 0.0) to 9.81×10^5 Ω cm (x = 0.4), and then decreased to 3.14×10^4 Ω cm (x = 0.8).

1 Introduction

Y-type hexagonal ferrites $Ba_2Me_2Fe_{12}O_{22}$, where Me represents a divalent ion such as cobalt, nickel and zinc, consist of S and T molecular unit having the unit cell formula 3(ST) [1]. Y ferrites were the first ferroxplana ferrites to be discovered, which have a preferred plane of magnetization perpendicular to the c-axis at room temperature. There is no five-coordinate site in the T-block, so the spin-orbit coupling contributes little to *K*. As a result, these ferrites have lager negative *K* values. Among these ferrites, Co_2Y has the highest magnetic anisotropy in room temperature. Co_2Y ferrite has the strong magnetic anisotropy field and high cut-off frequency, which is one order of magnitude higher than the traditional spinel [2–4]. Y-type hexagonal ferrites are qualified for various applications in modern information and communication processing devices, used as UHF soft magnetic material [5–10].

Widely used as high-frequency soft magnetic material, low initial permeability of Co_2Y cannot meet the development of electronic devices any more. In order to apply in more extensive electronic areas, it's necessary to use ion modification to improve properties of material. Cu^{2+} ion has similar radius as Fe^{2+} ion, and it is one of most effective ways to improve property of ferrites [11–15]. The melting point of CuO is 1026 °C, it melts during the sintering process and forms liquid phase, which could lower the sintering temperature and promote grain growth. Zhang et.al. [16] reported Cu substitution Z-type hexagonal barium ferrites, and the sintering temperature of ferrite has been lowered to 1050–1130 °C. It illustrated CuO additive could lower the sintering temperature about 150 °C. In ferrites, CuO substitution not only reduced the sintering temperature, but also adjusted the magnetic properties. In present work, we chose Cu^{2+} ions to substitute Co^{2+} ions of Co_2Y ferrite ($Ba_2Co_{2-x}Cu_xFe_{12}O_{22}$, x = 0.0, 0.2, 0.4, 0.6, 0.8) at low temperature (~1100 °C). Phase formation, microstructure, magnetic properties and DC resistivity of samples were investigated. The magnetism of effect of Cu-substitution on structure and property was discussed.

✉ Yingli Liu
lyl@uestc.edu.cn

[1] State Key Laboratory of Electronic Thin Films and Integrated Devices, University of Electronic Science and Technology of China, Chengdu 610054, China

2 Experiment procedure

Y-type hexagonal ferrites ($Ba_2Co_{2-x}Cu_xFe_{12}O_{22}$, x = 0.0, 0.2, 0.4, 0.6, 0.8) were prepared using solid-state reaction method. Analytic reagent grade raw materials $BaCO_3$, CuO, CoO, and Fe_2O_3, were mixed in a ball mill for 6 h, using stainless-steel balls and deionized water as media. The mixed powders were dried and pre-sintered at 1050 °C for 3 h in air. Then the powders were ball-milled again for 12 h in deionized water. After drying, powders were granulated by adding 8 wt% of polyvinyl alcohol (PVA) as a binder and pressed into 2–3 mm thick plates. Then the samples were sintered at 1100 °C for 4 h.

The phase compositions of the samples were determined using an X-ray diffractometer (XRD, DX-2700, Haoyuan Co.) with Cu Kα radiation. The microstructures of the samples were characterized using a scanning electron microscope (SEM, JEOL, JSM-6490). The bulk density was measured using an auto density tester (GF-300D, AND Co.) by Archimedes' principle. Magnetization hysteresis loops were measured using a vibrating sample magnetometer (VSM, MODEL, BHL-525). Complex magnetic permeability was determined by using a HP-4991B RF impedance analyzer. DC resistivity of samples (Ag-Ag contact coated onto both sides) was measured by two probe method using a digital super megohmmeter (DSM-8104).

3 Results and discussion

3.1 Phase formation

Figure 1 showed the XRD patterns of the samples with different compositions compared with the standard XRD spectrum of Y-type phase. All the diffraction peaks were matched with standard patterns, which confirmed that all the samples were in single phase with hexagonal structure and no impurity phase was present. When x = 0.0, well defined Co_2Y ferrite phase could be obtained. With Cu^{2+} ion adding, the peak intensity increased, which indicated that CuO addition could lower the sintering temperature and promoted the growth of crystalline grain. When the sintering temperature increased to 1100 °C, CuO began to wet and form liquid which spread across the surface of Co_2Y ferrite [17].

The melting CuO preferred to enter crystal lattice and occupy the lowest energy configuration. Hence, Cu-substitution not only modified properties of Co_2Y ferrite, but also lowered the sintering temperature.

Lattice constants (*a* and *c*) of sintered samples were calculated using different diffraction peaks in the diffraction patterns as per the hexagonal crystal, and variations of

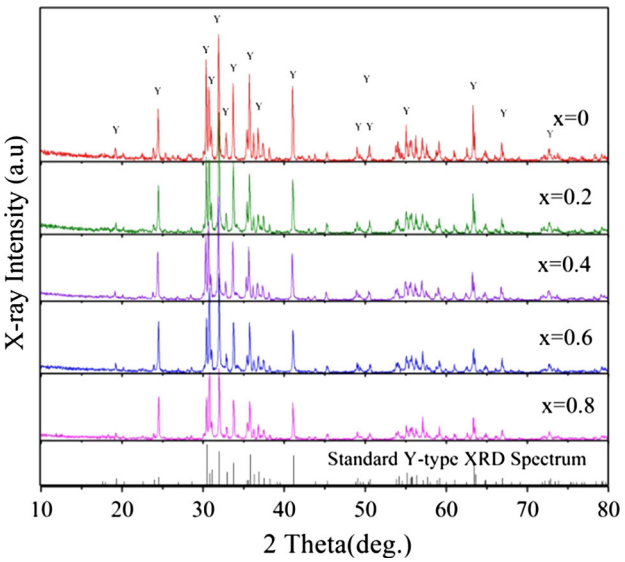

Fig. 1 XRD patterns of $Ba_2Co_{2-x}Cu_xFe_{12}O_{22}$ (x = 0.0, 0.2, 0.4, 0.6, 0.8) samples sintered at 1100 °C

lattice constants as a function of CuO content were shown in Fig. 2. There was a decrease in lattice constants *a* and *c* with CuO substitution from x = 0 to x = 0.8. First, the lattice constants (a = 0.587 nm, c = 4.356 nm) of pure Co_2Y ferrites were close to the theoretical values. In consideration of ionic radii of cations, the ionic radius of Cu^{2+} ion is 0.73 Å and that of Co^{2+} ion is 0.745 Å. Cu^{2+} substituted Co^{2+} therefore brought a lattice distortion and led to a decrease of the lattice constants.

3.2 Microstructure and densification

The cross-sectional SEM micrographs and bulk density of the sample were shown in Fig. 3. The microstructure of the samples was influenced by the variance of CuO contents. As shown in Fig. 3a, none substitute Co_2Y ferrite (x = 0.0)

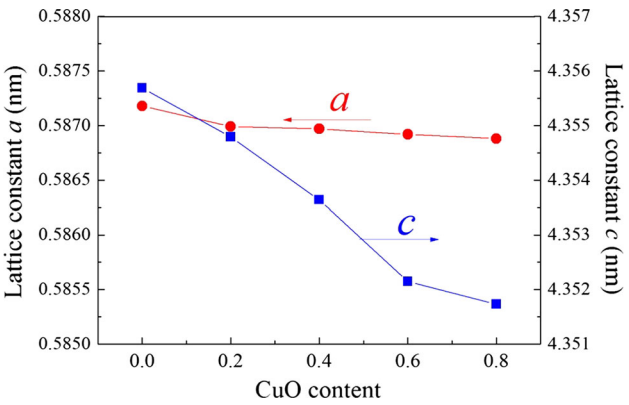

Fig. 2 Effects of CuO substitution upon lattice parameters of samples

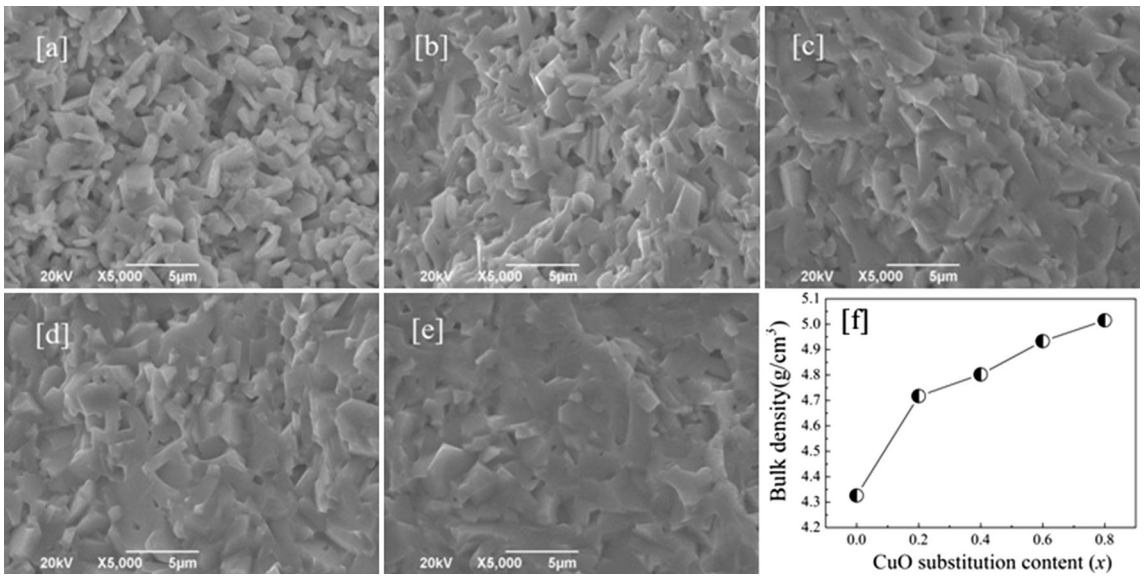

Fig. 3 SEM micrographs of the cross-sectional and bulk density of $Ba_2Co_{2-x}Cu_xFe_{12}O_{22}$ samples (**a** x = 0.0, **b** x = 0.2, **c** x = 0.4, **d** x = 0.6, **e**. x = 0.8, **f** bulk density)

presented plate-like grains, and had smaller average grain size and lower densification comparing with other samples. With CuO increasing, the grain size increased and densification enhanced, which led to increase of bulk density, as shown in Fig. 3f. CuO-substitute brought more compactly stacked and less pores between particles, which was ascribed to the appropriate segregation and volatilization of Cu [16]. When x = 0.8, part of the grain boundaries disappeared, and fewer pores left between particles and higher bulk density was enhanced.

As shown in Fig. 3f, bulk density of the samples increased, correspond to SEM images. The density increased with CuO content greatly. The density of pure Co_2Y sample was only 4.326 g/cm^3. CuO addition improved the density dramatically and maximum density reached 5.015 g/cm^3 when x = 0.8, which is 92.9% of the standard theoretical density (5.40 g/cm^3) [1].

3.3 Magnetic properties

Magnetic hysteresis loops of the samples were shown in Fig. 4. Figure 5 showed values of saturation magnetization (M_s) and coercivity (H_c) of samples. All the samples exhibited typical hysteresis behavior under applied magnetic field at room temperature with complete saturation magnetization from $\sim$H > 3000 Oe. This evidenced the magnetic nature of the samples. The theory saturation magnetization of pure Co_2Y ferrite was 34 emu/g [1]. In present experiment, when x = 0.0, the saturation magnetization was 31.7 emu/g. The loss of M_s was due to insufficient grain growth without CuO addition in 1100 °C. This result was consistent with previous analysis [17]. With

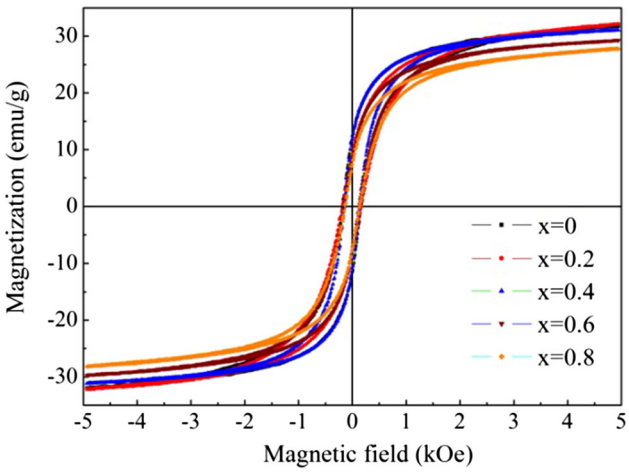

Fig. 4 M-H hysteresis loops of the samples in room temperature

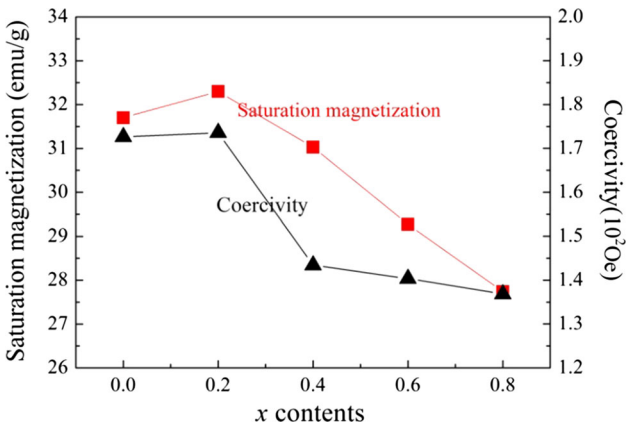

Fig. 5 Saturation magnetization and coercivity of $Ba_2Co_{2-x}Cu_xFe_{12}O_{22}$ (x = 0.2, 0.4, 0.6, 0.8) ferrite

CuO substitution, M_s increased from 31.7 emu/g (x = 0.0) to 32.3 emu/g (x = 0.2), and then decreased to 27.7 emu/g (x = 0.8).

In ferrites, the saturation magnetization is mainly come from total net magnetic moment (m) and chemical composition. The value of m of Co_2Y ferrite is $9.8\mu_B$ per unit formula. Co^{2+} ion has a marked preference for octahedral sites and carries a magnetic moment of $3.7\mu_B$. Among the octahedral sites of Y structure, there are one spin down octahedral sublattice $6C_{VI}$ (↓) and three spin up sublattices $3a_{VI}$(↓), 18 h_{VI}(↓) and $3b_{VI}$(↓). 0.9 cobalt ions are located in the only spin down octahedral sublattice, whilst the remnant 1.1 are supposed to be distributed among the spin up sublattices [18]. Magnetization in a ferrite comes from the total net magnetic moment between tetrahedral and octahedral sublattices which align in an antiparallel arrangement with respect to each other due to super exchange [19].

When CuO substituted Co_2Y ferrites, when x = 0.2, the increase of M_s was due to high densification and few pores between grains. With increasing of CuO, the decrease of M_s mainly came from the decrease of total magnetic moment. The magnetic moment of Cu^{2+} ions is $1.3\mu_B$, which is smaller than that of Co^{2+} ions ($3.7\mu_B$). Cu^{2+} ions distributed in the spin up octahedral sub lattices $3a_{VI}$, 18 h_{VI}, or $3b_{VI}$. The lower magnetic moment of Cu^{2+} ions in the vicinity of Co^{2+} ions diluted the strength of the super exchange interaction and reduced the total magnetic moment of ferrite. Thus, the saturation magnetization showed a downward trend with increase of CuO content after x = 0.2.

Coercivity (H_c) is the magnetic field intensity required to reduce the magnetization of a magnetic sample to zero after magnetization saturation, and it is the principle parameter used to distinguish between soft and hard magnetic materials. Pure Co_2Y-type barium ferrite is a soft magnetic material with an experimental maximum coercivity of about 377 Oe [1]. In the present study, a range of 172–136 Oe was obtained as shown in Fig. 5. When CuO substituted, coercivity dropped and the samples possessed better soft magnetic properties. Firstly, Cu^{2+} ion substitution for Co^{2+} ion weakened the magnetic planar anisotropy, which in turn reduced coercivity. Secondly, the different values of coercivity were related with the domain wall motion, which was affected by the grain size and could be enhanced by the increase of grain size. Lastly, lattice distortion and densification were another reason of coercivity change. Lattice distortion would decrease coercivity and high densification increased coercivity. Hence, the variation in coercivity may be due to the combined effects of ion composition, grain size, lattice distortion and densification.

The real (μ') and imaginary (μ'') part of magnetic permeability versus frequency for the CuO substitution $Co_{2-}Y$ ferrite were determined from the magnetic measurement. Figure 6 indicated the frequency dependence of complex permeability with different CuO content. With CuO content increasing, the value of μ' increased gradually at 0.1–1 GHz. Meanwhile, the μ'' increased slightly and kept a low value of under 0.25. Hence, the samples processed low magnetic loss (tanδ) (about 0.08) from 0.1 to 1 GHz.

Magnetic permeability of ferrites can be expressed by

$$\mu \propto \frac{M_s^2}{K_1 + \lambda_s \sigma}$$

where M_s stands for saturation magnetization, K_1 stands formagneto-crystalline anisotropy, λ_s stands for magnetostriction factor and σ stands for internal stress [8]. Hexagonal ferrites containing Co^{2+} ion inclines to exhibit planar anisotropy, such as Co_2Y, which has the highest magnetic anisotropy constant among hexagonal ferrites, with a $(K_1 + 2K_2)$ value of -2.6×10^5 Jm^{-3} [1]. The variation of saturation magnetization and anisotropy determined the variation permeability of the samples. Cu^{2+}

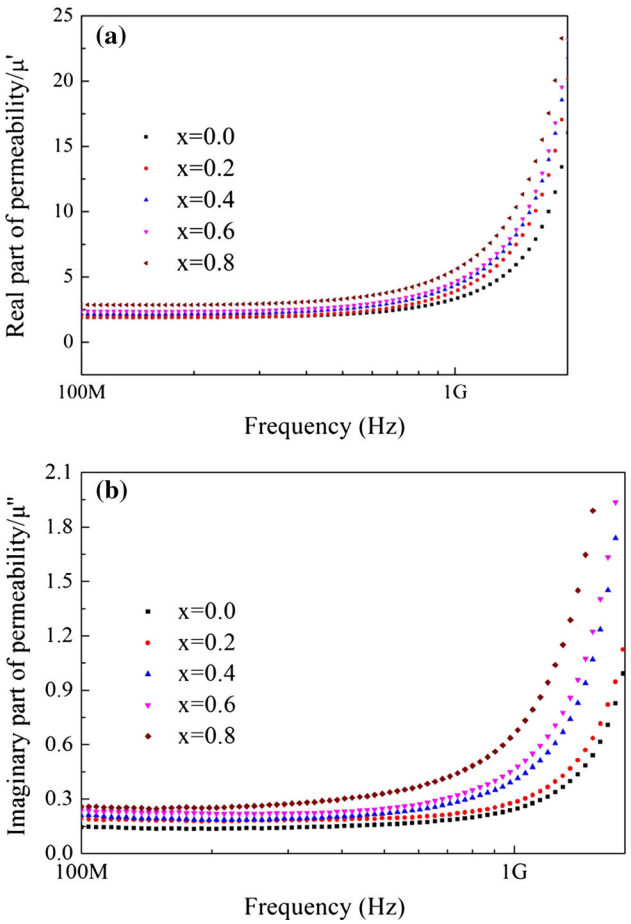

Fig. 6 Effect of CuO substitution for magnetic permeability of Co_2Y ferrite, **a** measured real part of μ' as function of field frequency, **b** measured imaginary part of permeability of μ'' as function of field frequency

ion substitution weakened the magnetic planar anisotropy, which in turn affected magnetic permeability. According to the discussion above, CuO substitution in Co_2Y ferrite reduced saturation magnetization as well as the magnetic anisotropy. The increase of μ' revealed that the declining of M_s was shaper than that of K_1.

In ferrite, permeability is relate to microstructure [8]. In our experiment, appropriate amount of CuO led to more compactly stack and larger grains, which facilitated magnetization rotation. Meanwhile, less pores between boundaries made the domain wall motion easier. Besides, the liquid phase of CuO helped to form uniform microstructure that cut down the internal stress, which increased magnetic permeability. Thus, with CuO increasing from 0.0 to 0.8, real part of magnetic permeability increased gradually. For none substitution sample ($x = 0.0$), the immaturity of grain growth and low bulk density caused low magnetic permeability.

3.4 DC resistivity

The DC resistivity of the samples with different CuO substitution contents was shown in Fig. 7. The radius and thickness of the samples were measured then sliver was coated on both sides. Using two probe methods, resistance of the samples were measured by digital super megohmmeter (DSM-8140). The DC resistivity of the samples can be obtained by

$$R = \rho \frac{s}{l}$$

The room temperature DC resistivity first increased from 3.65×10^5 Ω cm ($x = 0.0$) to 9.81×10^5 Ω·cm ($x = 0.4$) with CuO increasing, and then dropped to 3.14×10^4 Ω·cm ($x = 0.8$). The dominant conduction mechanism in ferrites is electron hopping between Fe^{2+} ion and Fe^{3+} ion at two interstitial sites. According to above discussion, Cu^{2+} ions preferentially occupy octahedral sites. The existence of Cu^{2+} ion would create internal stress and inhibit the electron hopping, and this led to the increase of DC resistivity [16]. When CuO content further increased, some grain boundaries disappeared and fewer pores left between particles, as shown seen from the SEM images. It has been reported by Yang Bai et al. [20] that deficiencies tend to gather at grain boundaries to form a more resistive surface. When some grain boundaries disappeared in the samples, it might lead to the decrease of resistivity. Besides, the increasing electrical resistivity was attributed to increasing number of pores by Mukhtar et al. [21]. Pores were thought to hinder the motion of charge carriers from their work. Hence, the decrease of pores could make electron hopping easier and cause the loss of resistivity. The decrease of grain boundaries and pores led to the decrease of resistivity.

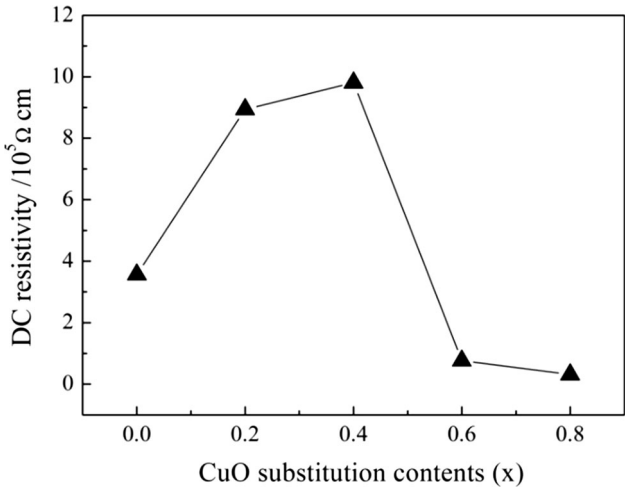

Fig. 7 The DC resistivity of the samples with different CuO substitution contents

4 Conclusions

In the present study, we have investigated the effect of CuO substitution upon the structural and magnetic properties of Co_2Y barium ferrite. Single phase CuO substituted barium ferrites have been successfully synthesized at a low sintering temperature of 1100 °C. CuO substituted Y-type ferrites were suitable for high frequency applications because the magnetic permeability increased and remained steady from 100 to 700 MHz while the magnetic loss increased a little. This substitution not only improved microstructure but also brought changes to other magnetic properties. The saturation magnetization and magnetic anisotropy decreased as Cu^{2+} ion substituted Co^{2+} ion. DC resistivity of the samples reached maximum value 9.81×10^5 Ω cm at $x = 0.4$ and then decreased. It would be necessary to improve the DC resistivity in the subsequent research in order to cut down eddy current loss in high frequency.

Acknowledgments This work was supported by the Natural Science Foundation of China under Grant Nos. 61371053 & 5162036, and by the Innovation fund of CETC under No. JJ120304, and by the National High-tech R&D Program of China (863 Program, Grant No. 2015AA034102), and by the Fundamental Research Funds for the Central Universities under No. A03013023601061.

References

1. R.C. Pullar, Hexagonal ferrites: a review of the synthesis, properties and applications of hexaferrite ceramics. Prog. Mater Sci. **57**, 1191–1334 (2012)

2. H. Zhang, Z. Ma, J. Zhou, Z. Yue, L. Li, Z. Gui, Preparation and investigation of $(Ni_{0.15}Cu_{0.25}Zn_{0.60})Fe_{1.96}O_4$ ferrite with very high initial permeability from self-propagated powders. J. Magn. Magn. Mater. **213**, 304–308 (2000)
3. J. Mürbe, J. Töpfer, High permeability Ni–Cu–Zn ferrites through additive-free low-temperature sintering of nanocrystalline powders. J. Eur. Ceram. Soc. **32**, 1091–1098 (2012)
4. K.O. Low, F.R. Sale, The development and analysis of property—composition diagrams on gel-derived stoichiometric NiCuZn ferrite. J. Magn. Magn. Mater. **256**, 221–226 (2003)
5. Y. Bai, J. Zhou, Z. Gui, L. Li, Magnetic properties of Cu, Zn-modified Co_2Y hexaferrites. J. Magn. Magn. Mater. **246**, 140–144 (2002)
6. Y. Bai, J. Zhou, Z. Gui, Z. Yue, L. Li, Complex Y-type hexagonal ferrites: an ideal material for high-frequency chip magnetic components. J. Magn. Magn. Mater. **264**, 44–49 (2003)
7. Y. Bai, J. Zhou, Z. Gui, L. Li, Frequency dispersion of complex permeability of Y-type hexagonal ferrites. Mater. Lett. **58**, 1602–1606 (2004)
8. Y. Bai, J. Zhou, Z. Gui, L. Li, L. Qiao, The physic properties of Bi–Zn codoped Y-type hexagonal ferrite. J. Alloys Compd. **450**, 412–416 (2008)
9. Y. Bai, J. Zhou, Z. Gui, L. Li, An investigation of the magnetic properties of Co_2Y hexaferrite. Mater. Lett. **57**, 807–811 (2002)
10. Z. Li, M. Chua, Z. Yang, Studies of static, high-frequency and electromagnetic attenuation properties for Y-type hexaferrites $Ba_2Cu_xZn_{2-x}Fe_{12}O_{22}$ and their composites. J. Magn. Magn. Mater. **382**, 134–141 (2015)
11. J.-Y. Hsu, W.-S. Ko, H.-D. Shen, C.-J. Chen, Low temperature fired NiCuZn ferrite. IEEE Trans. Magn. **30**, 4875–4877 (1994)
12. J. Nam, H. Jung, J. Shin, J. Oh, The effect of Cu substitution on the electrical and magnetic properties of NiZn ferrites. IEEE Trans. Magn. **31**, 3985–3987 (1995)
13. S. Kračunovska, J. Töpfer, Synthesis, sintering behavior and magnetic properties of Cu-substituted Co2Z hexagonal ferrites. J. Mater. Sci.: Mater. Electron. **22**, 467–473 (2011)
14. Y. Bai, J. Zhou, Z. Yue, Z. Gui, L. Li, Magnetic properties of composite Y-type hexagonal ferrites in a direct current magnetic field. J. Appl. Phys. **98**, 063901 (2005)
15. Y. Bai, J. Zhou, Z. Gui, L. Li, Effect of substitution on magnetization mechanism for Y-type hexagonal ferrite. Mater. Sci. Eng., B **103**, 115–117 (2003)
16. H. Zhang, J. Zhou, Y. Wang, L. Li, Z. Yue, X. Wang, Z. Gui, Investigation on physical characteristics of novel Z-type $Ba_3Co_{2(0.8-x)}Cu_{0.40}Zn_{2x}Fe_{24}O_{41}$ hexaferrite. Mater. Lett. **56**, 397–403 (2002)
17. Y. Bai, W. Zhang, L. Qiao, J. Zhou, Low-fired Y-type hexagonal ferrite for hyper frequency applications. J. Adv. Ceram. **1**, 100–109 (2012)
18. G. Albanese, M. Carbucicchio, A. Deriu, G. Asti, S. Rinaldi, Influence of the cation distribution on the magnetization of Y-type hexagonal ferrites. Appl. Phys. **7**, 227–238 (1975)
19. J. Li, H. Zhang, V. Harris, Y. Liao, Y. Liu, Ni–Ti equiatomic co-substitution of hexagonal M-type Ba $(NiTi)_xFe_{12-2x}O_{19}$ ferrites. J. Alloys Compd. **649**, 782–787 (2015)
20. Y. Bai, J. Zhou, Z. Gui, L. Li, Electrical properties of non-stoichiometric Y-type hexagonal ferrite. J. Magn. Magn. Mater. **278**, 208–213 (2004)
21. M. Ahmad, F. Aen, M. Islam, S.B. Niazi, M. Rana, Structural, physical, magnetic and electrical properties of La-substituted W-type hexagonal ferrites. Ceram. Int. **37**, 3691–3696 (2011)